

Article

Human-Altered Water and Carbon Cycles in the Lake Yangzong Basin since the Yuan Dynasty

Huayong Li ¹, Yuxue Jing ¹, Hucai Zhang ^{2,*} , Xuanxuan Shang ³, Lizeng Duan ², Huayu Li ², Donglin Li ⁴ and Zhuohan Li ¹

¹ School of Resource Environment and Tourism, Anyang Normal University, Anyang 455000, China; lihuayong2010@hotmail.com (H.L.); 18703683267@163.com (Y.J.); 19837268129@163.com (Z.L.)

² Institute for Ecological Research and Pollution Control of Plateau Lakes, School of Ecology and Environmental Science, Yunnan University, Kunming 650500, China; duanlizeng2019@ynu.edu.cn (L.D.); xihuayu@163.com (H.L.)

³ School of Media and Communications, Anyang Normal University, Anyang 455000, China; fuyuetegong@126.com

⁴ Institute of Culture and Tourism, Qujing Normal University, Qujing 655011, China; lidonglin@mail.qjnu.edu.cn

* Correspondence: zhanghc@ynu.edu.cn

Abstract: Due to the dual influence of climate change and human activities, the water cycle patterns in the lakesheds of the Yunnan karst plateau are undergoing significant changes, leading to increasingly prominent ecological issues. In the history of Lake Yangzong, an artificial water-diversion channel was excavated, altering the lake basin structure. Human activities have intensified, posing severe challenges to water resource supply and water security in recent decades. To investigate the significant increase in human activities, the temporal and phase changes, and the resulting transformation of the water and carbon cycles in the Lake Yangzong basin, we applied X-ray fluorescence spectroscopy (XRF) to scan elements continuously in a 10.2 m sediment core from this lake. By combining correlation analysis, principal component analysis (PCA), core chronology, and total organic carbon (TOC) content, we reconstructed the historical sequence of geochemical element contents in the Lake Yangzong catchment over the past 13,000 years. The results show that PC1 and PC2 contribute 78.4% and 10.3%, respectively, suggesting that erosion intensity is the main factor influencing the lake sedimentation process. From 13,400 to 680 cal a BP (calibrated years before the present), the sedimentation process in Lake Yangzong was mainly controlled by climatic conditions, with vegetation degradation during cold periods and relatively high erosion intensity in the watershed. During the Yuan dynasty, a province was established by the central government in Yunnan, promoting settlement and attracting a large number of immigrants from other provinces to Yunnan. Human activities in the Lake Yangzong basin began to intensify, surpassing natural changes and becoming the dominant force influencing the sedimentation process. In the Ming and Qing dynasties, the population and cultivated land area in Yunnan further increased, resulting in the significant exacerbation of erosion and soil loss in the watershed due to vegetation destruction. In the year 1388, the Tangchi Canal was excavated, transforming Lake Yangzong to an outflow lake, causing Ca²⁺ to be lost through the Tangchi Canal and preventing the formation of precipitation due to oversaturation. The research results indicate that human activities in the Lake Yangzong area have intensified since the Yuan dynasty, leading to increased erosion intensity. The excavation of the outflow canal transformed Lake Yangzong from an inland lake basin into an outflow state, simultaneously generating a significant transformation in the water and carbon cycling patterns in the watershed.

Keywords: Lake Yangzong catchment; XRF core scanning; the Holocene; water–carbon cycle; catchment erosion; human activities



Citation: Li, H.; Jing, Y.; Zhang, H.; Shang, X.; Duan, L.; Li, H.; Li, D.; Li, Z. Human-Altered Water and Carbon Cycles in the Lake Yangzong Basin since the Yuan Dynasty. *Water* **2024**, *16*, 1271. <https://doi.org/10.3390/w16091271>

Academic Editor: Carmen Teodosiu

Received: 23 March 2024

Revised: 26 April 2024

Accepted: 26 April 2024

Published: 29 April 2024



Copyright: © 2024 by the authors. Licensee MDPI, Basel, Switzerland. This article is an open access article distributed under the terms and conditions of the Creative Commons Attribution (CC BY) license (<https://creativecommons.org/licenses/by/4.0/>).

1. Introduction

In the Yunnan Plateau, there are 30 lakes with a surface area of over 1 km². Among these, nine lakes have a surface area greater than 30 km², making this region one of the areas in China with a dense distribution of lakes. Predominantly, these lakes are karst tectonic-fault lakes, with basins that are mostly closed or semi-closed [1]. As crucial components of the terrestrial hydrosphere and regional hydrological centers, lakes participate in the water cycle at various scales, reflecting changes in the regional climate environment and serving as excellent indicators of climate change [2,3]. Simultaneously, the plateau lake basins are major population and urban agglomerations, bearing the highest economic and environmental loads [4]. Under the combined effects of climate change and human activities, the lakes on the Yunnan Plateau are experiencing varying degrees of change in water level [5,6], area [4], number [7], and water quality [8]. Especially since the advent of the Anthropocene [9–11], human activities have surpassed natural variations [12], becoming the dominant force affecting lake basin erosion [13], water volume [4], and water quality [14]. However, prior to 1950, human agricultural activities had already significantly impacted the environment of typical plateau lake basins in Yunnan [15], yet the onset, methods, intensity, and processes of their impact remain unclear. The timing of when human activities in different lake basins surpassed natural forces and became the primary geological force shaping the surface environment also varies [16,17]. Identifying signals of human activity from regional environmental evolution records spanning millennia or longer and further reconstructing the history of human activity and its environmental effects in lake basins are necessary [18].

Lake sediments serve as a product and archive of the interactions among various spheres within a lake basin under natural and anthropogenic influences, preserving rich information on regional tectonic activities, climate environmental changes, and human activities [19–21]. They are characterized by minimal disturbance from human activities, continuous and complete deposition, and high resolution, making them excellent proxies for studying the evolution of human–environment relationships in past lake basins [22]. Surface geochemical elements within lake basins are continuously leached and transported through physical and chemical weathering processes, eventually accumulating in lake sediments. Hence, the variations of elements in lake sediments can be used to reconstruct the climatic environment and hydrological evolution history of the basin [23–25]. X-ray fluorescence (XRF) spectroscopy, by conducting continuous scans on the core surface, acquires information on the abundance and composition of geochemical elements in sediment profiles. This method is advantageous for its rapidity, non-destructiveness, high resolution, and minimal sample-preparation requirements [26–28] and has been increasingly applied in marine and lacustrine drilling as well as speleothem studies, yielding a series of high-resolution climate environmental records [29–32]. Comparative studies with ICP-AES elemental quantitative analysis methods have confirmed the reliability and credibility of XRF core scanning technology. Through a series of data transformations, it can reveal changes in geochemical elements in cores with high resolution [33–36]. In recent years, XRF technology has been widely applied in lake sediment research, achieving significant results regarding sediment provenance analysis, the identification of paleofloods and marker climatic events, regional precipitation reconstruction, the inversion of watershed weathering and erosion history, watershed hydrological characteristics, and environmental evolution [37–40]. Compared with using XRF to reveal paleoenvironmental changes and natural disaster events [41–43], this study focuses more on the interactions between the Lake Yangzong basin ecosystem and human activities driven by historical border-governance policies.

Lake Yangzong, situated on the Yunnan–Guizhou Plateau in the southwest of China, experiences a subtropical plateau monsoon climate, characterized by distinct dry and wet seasons. This region boasts a lengthy history of basin development, featuring continuous and stable lake deposits that provide clear signals of both climatic fluctuations and anthropogenic activities [3,44]. Historically, Lake Yangzong was a closed lake until AD 1388 when the Tangchi Canal was constructed to divert lake water for agricultural irrigation and transform it into an outflow lake. However, it is unclear when human activities in the Lake Yangzong basin exceed

natural forces and how they impact the regional water and carbon cycling patterns. Therefore, this study focuses on a 10.2 m long sedimentary core from Lake Yangzong, establishing a reliable chronological framework using seven AMS-14C age control points. Employing XRF core continuous scanning technology, this research obtains high-resolution geochemical element records. In conjunction with variations in total organic carbon (TOC), this study reconstructs the environmental evolution and watershed erosion processes in the region since the last glacial period. It aims to investigate the onset of and mechanisms behind significant alterations in geochemical element behavior and hydrological cycle patterns within the Lake Yangzong basin, attributing these changes to human activities.

2. Materials and Methods

2.1. Study Area

Lake Yangzong, located in the eastern part of the Yunnan Plateau (Figure 1), covers an area of 31 km² with a watershed area of 192 km². It has a maximum depth of 31 m and an average depth of 20 m, making it the third deepest lake in Yunnan. Lake Yangzong is a typical faulted deep-water lake. The outcrops of its watershed are primarily composed of Permian, Carboniferous, and Devonian limestone and basalt, followed by sandstones from the Cambrian, Jurassic, and Silurian periods. The areas of the basin's northern and southern shores predominantly expose Quaternary fluvial-lacustrine facies [45]. The region experiences a subtropical plateau monsoon climate, with an annual average rainfall of 900 mm, characterized by distinct wet and dry seasons. The lake's water is mainly replenished by precipitation. In addition to the rainy season's runoffs, the primary sources include the Yangzong River, Qixing River, and other seasonal streams from the east and west sides, with the Tangchi Canal on the northeast side serving as the only outlet. The predominant soil type in the watershed is lateritic soil, which has a high dispersion coefficient and is relatively light in texture [46]. The vegetation in the Lake Yangzong watershed is characteristic of the subtropical zones on the Yunnan Plateau, dominated by evergreen broad-leaved forests and Yunnan pine forests, with a significant proportion of farmland [3]. Since the mid-20th century, human activities in the watershed have intensified, with rapid development in industry, agriculture, and tourism, leading to a noticeable deterioration of the ecological environment [47].

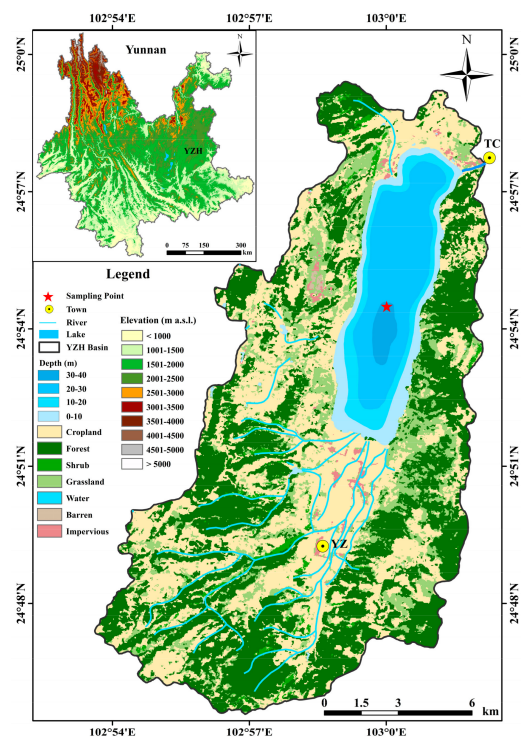


Figure 1. Land use map of the catchment of Lake Yangzong and the location of YZH-1 core. URL (<https://zenodo.org/records/8176941>, accessed on 1 December 2022).

2.2. Coring

In July 2013, at a water depth of 23 m in Lake Yangzong (24°54'42" N, 103°0'7" E, Figure 1), nine deep rock cores were obtained using an Austrian UWITEC water sampling platform and a piston corer with overlapping penetration depths. Based on the penetration depths and elemental scanning results, a continuous lake sediment core of 10.2 m was assembled, designated as YZH-1 (Yangzonghai-1).

2.3. Age Control

After the core samples were brought back to the laboratory and split open, abundant terrestrial plant debris (such as leaves and wood chips) was found in the sediment, which could help avoid potential carbon reservoir effects [48], making it an excellent material for ¹⁴C dating. Seven samples of wood chips and leaf debris were selected at depths of 77 cm, 341 cm, 428 cm, 53 cm, 738 cm, 966 cm, and 1002 cm in the core and were dated using AMS-¹⁴C at the Key Laboratory of Heavy Ion Physics of the Ministry of Education at Peking University [3]. We calibrate the ¹⁴C ages using the newest IntCal14 in this paper [49].

2.4. XRF Core Scanning

Half of the core was scanned for chemical elements using the Dutch Avaa-tech XRF core scanner, with a scan area of 5 mm (width) × 10 mm (length) and a scan time of 30 s. The top 0–120 cm was scanned at a resolution of 5 mm, while the lower section from 120–1020 cm was scanned at intervals of 10 mm, resulting in a total of 1131 reliable data sets. To ensure the accuracy of the analysis, this study focuses on the analysis of nine elements with strong XRF scan signals, including Fe, Mn, Ti, Al, Si, Zr, Sr, Ca, and Rb. These nine elements have relatively high contents in lake sediment, with small measurement errors, and clear environmental indicative significance [39].

2.5. TOC Analysis

The TOC content was determined using loss-on-ignition [50]. Initial sample weights were ~3.00 g and were manually pulverized using an agate mortar pestle. Subsequently, the samples were dried at 105 °C for 2 h to ensure complete dryness before determining the total organic carbon. The samples were then heated at 550 °C for 4 h, and the loss in mass represents the TOC content. The XRF core scanning and TOC analysis were conducted at the Key Laboratory of Plateau Lake Ecology and Global Change at Yunnan Normal University.

2.6. Numerical Analysis

The software used for both correlation analysis and principal component analysis (PCA) was the R language (version 4.2.1, URL (<https://www.r-project.org/>), accessed on 17 April 2024). Prior to the analysis, all data were standardized utilizing the 'factoextra' and 'FactoMineR' R packages.

3. Results

3.1. Lithology and Chronological Model

The YZH-1 core from Lake Yangzong mainly consists of clayey silty sand. The top 62 cm is brownish-red clayey silty sand, followed by a layer of light-gray silty sand from 62 to 392 cm and a lower layer of dark-gray sandy silty sand from 392 to 1020 cm. The age framework of the Lake Yangzong drilling core was established using AMS-¹⁴C dating data from seven wood and leaf samples, along with the set top age of the core (−63 cal a BP (calibrated years before the present)). The age boundary at the bottom of the core reaches 13,300 cal a BP, with an average sedimentation rate of 0.76 mm a^{−1} (Figure 2).

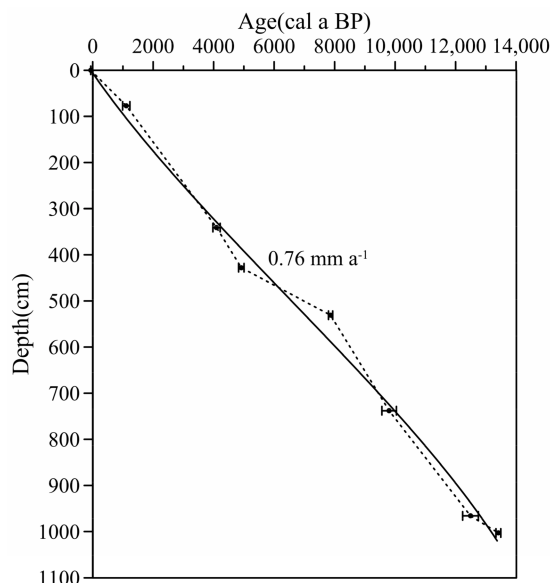


Figure 2. The age-depth model of YZH-1 core.

3.2. Correlation Analysis

The correlation results of the elements in the Lake Yangzong sediment (Table 1) show that Fe, Ti, Rb, and Zr have significant positive correlations, with correlation coefficients (R values) of 0.9 or higher between any two of them. Al and Si show a high correlation, both being rock-forming elements generally enriched in exogenous detrital clay minerals. Si can be used to reveal the strength of runoff in the watershed [50]. Sr and Ca show positive correlations with each other ($R = 0.656^{**}$) and negative correlations with other elements. During chemical weathering, Ca and Sr are easily leached and can form isomorphous minerals through mutual replacement; hence, they exhibit a strong correlation. Mn shows good correlations with Fe and Ti, weaker correlations with Al and Si, and negative correlations with Ca and Sr.

Table 1. The results of correlation analysis of main elements of YZH-1 core.

	Fe	Mn	Si	Al	Ca	Ti	Rb	Sr	Zr
Fe	1								
Mn	0.775 **	1							
Si	0.486 **	0.177 **	1						
Al	0.834 **	0.527 **	0.838 **	1					
Ca	−0.870 **	−0.681 **	−0.140 **	−0.567 **	1				
Ti	0.983 **	0.732 **	0.489 **	0.832 **	−0.856 **	1			
Rb	0.939 **	0.673 **	0.399 **	0.773 **	−0.897 **	0.924 **	1		
Sr	−0.736 **	−0.457 **	−0.508 **	−0.699 **	0.656 **	−0.720 **	−0.685 **	1	
Zr	0.955 **	0.715 **	0.380 **	0.761 **	−0.905 **	0.957 **	0.968 **	−0.663 **	1

Note: ** correlation is significant at the 0.01 level.

3.3. Principal Component Analysis

Principal component analysis was conducted on the elemental data of Fe, Mn, Ti, Al, Si, Zr, Sr, Ca, Rb, etc., obtained from the XRF scanning of the YZH-1 sediment core. The results show that there are two significant PCA axes influencing the behavior of elements in Lake Yangzong, explaining 78.4% and 10.3% of the element data (Figure 3), with a cumulative variance accounting for 88.7% of the total variance, which can effectively explain the information in the original data. In the PCA biplot of the elements, the magnitude and proximity to the axis of the loadings on the component axis reflect the strength of the element responses. The longer the distance and the closer to the axis, the greater the

influence of the element, and elements that are closer to each other on the plot denote a more significant relationship between them.

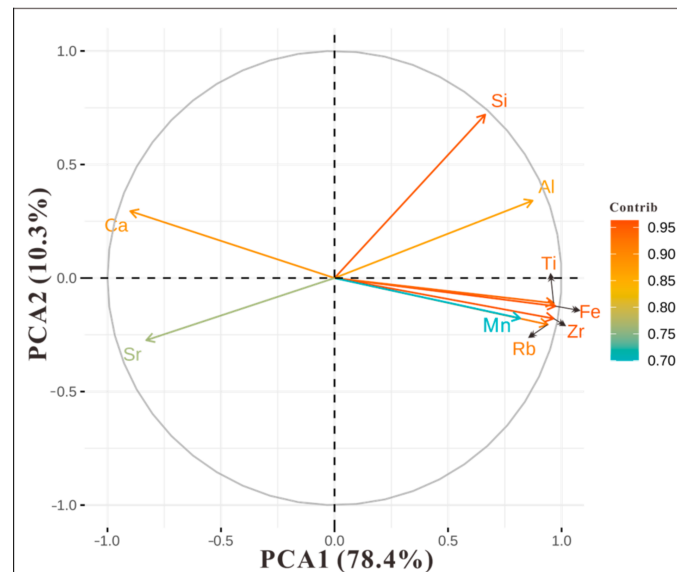


Figure 3. Biplot of elements PCA axis 1 and 2.

Axis 1 is mainly composed of terrigenous detrital elements such as Fe, Ti, Rb, Zr, Mn, Si, and Al in the positive direction, while Ca and Sr are predominant in the negative direction, typically coexisting in lacustrine secondary minerals. Axis 2 is characterized by Si, Al, and Ca elements in the positive direction, and Fe, Ti, Rb, Zr, Mn, and Sr elements in the negative direction. Figure 3 shows that axis 1 primarily reflects the variation between exogenous input detrital minerals and authigenic minerals in the lake, while PC2 accounts for only 10.3% of the variance in the elements, which is not statistically significant.

4. Discussion

4.1. Indication of XRF Core Scanning Elements and PCA

The correlation is controlled by the geochemical behavior of elements in the surface environment; high correlations between different elements indicate that they have the same source and consistent occurrence conditions [51]. High Fe content values typically occur in fine-grained sediment layers, suggesting the overall erosion intensity of the watershed; Ti, as a relatively inert element, is mainly influenced by physical weathering and regional precipitation changes and can be used as an indicator of detrital minerals in sediments; and Zr is a highly stable chemical element, mostly existing in the form of zircon in coarser-grained terrestrial detritus [52]. This group of elements represents terrestrial detritus and comes from relatively stable external inputs, with changes in their content in sediments mainly influenced by weathering and erosion intensity in the watershed. Mn is often dissolved, but under oxidizing conditions, it is oxidized into insoluble oxides and preserved in sediments [53].

As the principal component analysis shows, the elements Fe, Ti, Rb, Zr, and Mn are shown to be distantly located, close to the main axis, and near each other, suggesting a significant and influential relationship among these elements, the contributions of which are greater than 0.7 in PC1, representing exogenous detrital materials and reflecting the erosion intensity in the Lake Yangzong basin, which is controlled by a combination of regional precipitation, vegetation conditions, and human-activity intensity.

The contributions of Ca and Sr elements in the negative direction of principal axis 1 are both ~0.8. The characteristic behavior of the two elements is easy migration, with them ultimately entering the lake water after leaching and filtration during the weathering process in the lake basin [29]. Subsequently, they undergo endogenous substance generation within the lake through chemical and biological processes that, therefore, indicate the

endogenous mineral deposition generated by physicochemical and biological processes in Lake Yangzong, with the deposition amount ultimately controlled by climatic conditions (primarily temperature and precipitation) and the structure of the lake basin [54].

4.2. The Indicative Significance of TOC

It is commonly believed that the TOC contents reflect the level of primary productivity in lake watersheds [55,56], providing integrated information on the biomass from both internal and terrestrial sources, and, thus, are closely related to climatic conditions. High values correspond to periods of warm and humid climate with increased primary productivity, while low values correspond to periods of deteriorating environmental conditions [57]. After the onset of human activities, TOC primarily reflects changes in human activity types and intensities within the lake watershed [19,36]. However, the TOC content of core YZH-1 from Lake Yangzong shows a strong positive correlation with PC1 (Figure 4), indicating that it is controlled by changes in watershed erosion intensity resulting from the dual effects of climatic conditions and human activities. This suggests that TOC content indicates the input of organic matter in the watershed rather than the level of primary productivity [58,59].

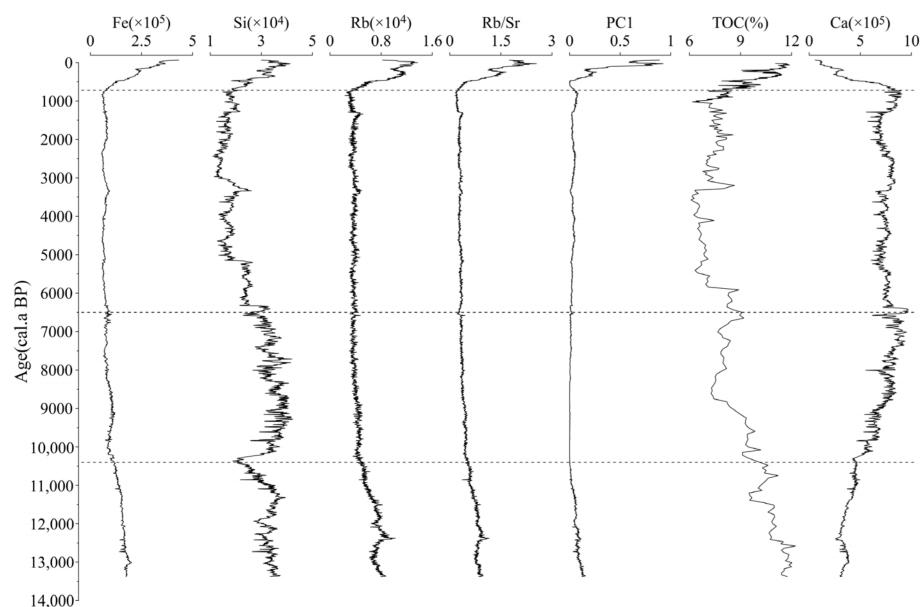


Figure 4. Proxies variations in the core sediment of Lake Yangzong.

4.3. Human–Earth System Evolution in Lake Yangzong Basin during the Holocene

Through correlation analysis and principal component analysis of the XRF scanning elements of the YZH-1 core sediment from Lake Yangzong, the sediment elements can be classified into two categories. Elements such as Fe, Ti, Rb, Zr, and Mn represent terrestrial detrital materials, reflecting the erosion intensity of the Lake Yangzong basin. Elements Ca and Sr represent endogenous materials produced by chemical and biological processes within the lake. The correlation between TOC content and elements like Fe is high, indicating the input of terrestrial detritus and organic residues in the basin. As shown in Figure 4, during the Last Glacial Termination period (13,400–10,400 cal a BP), the sediment in Lake Yangzong showed higher levels of terrestrial detrital elements like Fe and TOC, both of which exhibited a decreasing trend, while the Ca content was lower with a fluctuating increasing trend, revealing poor climatic conditions characterized by cold temperatures [60], vegetation degradation in the basin, severe surface erosion, and reduced precipitation of calcium carbonate in the lake water. From 10,400 to 680 cal a BP, the overall period was in the Holocene warm period, with significantly higher temperatures and precipitation compared to the cold periods [30], reflecting very low and stable erosion intensity in the basin. The TOC content also continued to decrease and remained at low

levels, suggesting high vegetation cover and low erosion intensity in the Lake Yangzong basin during this period. The variation in Ca content was completely opposite to PC1, showing an initial increase in volatility followed by a stable period. During this time, the average Ca content was the highest, implying an increase in the lake autochthonous carbonates under high-temperature climatic conditions [24]. The characteristics of the changes in XRF scanning elements and TOC content in the Lake Yangzong sediments show that the fluctuations in element and organic-matter content in the above two stages correspond to the stages of climate evolution, mainly controlled by climate and the resulting surface vegetation succession, with human activity signals being insignificant and having a very weak impact on the vegetation cover and erosion intensity in the basin.

4.4. Transformation of Water and Carbon Cycle in the Lake Yangzong Basin since Yuan Dynasties

Since 680 cal a BP (AD 1270), there has been a sudden increase in the intensity of the primary component elements, with a corresponding trend in TOC content (Figure 4), indicating a sharp degradation of vegetation [3] in the region and a significant increase in erosion intensity (Figure 5a). The surface of the basin is rich in elements such as Fe and Ti, with large amounts of red soil being lost to the lake basin (Figure 5b–d), depositing a layer of approximately 60 cm thick red clay at the top of the borehole (Figure 5e). In 1274, the Yuan dynasty established a provincial government in Yunnan and implemented a system of garrison farming, leading to a period of rapid population growth and the expansion of cultivated land in the region [61]. Extensive garrison farming caused severe damage to vegetation, especially in basin areas where land was depleted, forcing later farmers to develop steep mountainous areas and intensifying soil erosion [62]. Subsequently, the Ming and Qing dynasties largely continued the border governance policies of the Yuan dynasty, with increasing exchanges between Yunnan and the mainland resulting in a continuous increase in population and cultivated land [63] and further exacerbating erosion in the basin. The abnormal increase in the content of primary component elements and TOC in sediment records from Yangzonghai over the past 700 years reflects the tense relationship between humans and the environment during this period.

Approximately 600 years ago (late Yuan to early Ming dynasty), the Ca element content rapidly decreased, reaching near zero at the top of the drill hole (Figure 5a), with an average content representing the lowest stage in the past 13,300 years (Figure 4). During this period, the fluctuation and variation rate of Ca element content (mainly in the form of calcium carbonate [64]) exceeded any climate stage since the last ice melt period, which cannot be explained solely by climate control models [54]. Lake Yangzong originally had no outflow and was an endorheic lake, where calcium carbonate precipitation was controlled mainly by temperature-controlled models. In the year 1388 (562 cal a BP), the Tangchi Canal was excavated to divert lake water for the irrigation of farmland. The water flowed out from the Tangchi outlet on the northeast side, passed through Yiliang Dam, and entered the Nanpan River of the Pearl River system. Since then, Lake Yangzong has transformed from an endorheic lake to an exorheic lake, leading to significant changes in the water circulation pattern and hydrological environment of the lake. The lake water shifted from evaporation consumption to external discharge and evaporation consumption, causing the loss of Ca^{2+} and HCO_3^- through the Tangchi Canal, making it difficult to reach supersaturation, thereby resulting in a rapid and substantial decrease in calcium carbonate precipitation [52].

Although there has been evidence indicating human activities in the lake basins of central Yunnan Province during the Neolithic and Bronze Ages [65–68], this study reveals that the timing of when human activities in the Lake Yangzong basin surpassed natural changes and became a dominant force in shaping the surface landscape is relatively late, beginning in the Yuan dynasty. This transformation was driven by the proactive frontier policies of the Yuan dynasty. Since the Yuan dynasty, the change in border governance policies has led to a continuous increase in the population of the region, with a shift in land-use structure from forests to farmland and settlements. This has resulted in a significant decrease in the carbon sequestration capacity of the Lake Yangzong basin [69]. Intense

erosion processes within the basin may lead to the migration of organic matter to the lake basin, potentially accompanied by partial oxidation and decomposition, making the Lake Yangzong basin a potential carbon source [70,71]. So, in this sense, the Anthropocene in the Lake Yangzong basin began in the Yuan dynasty.

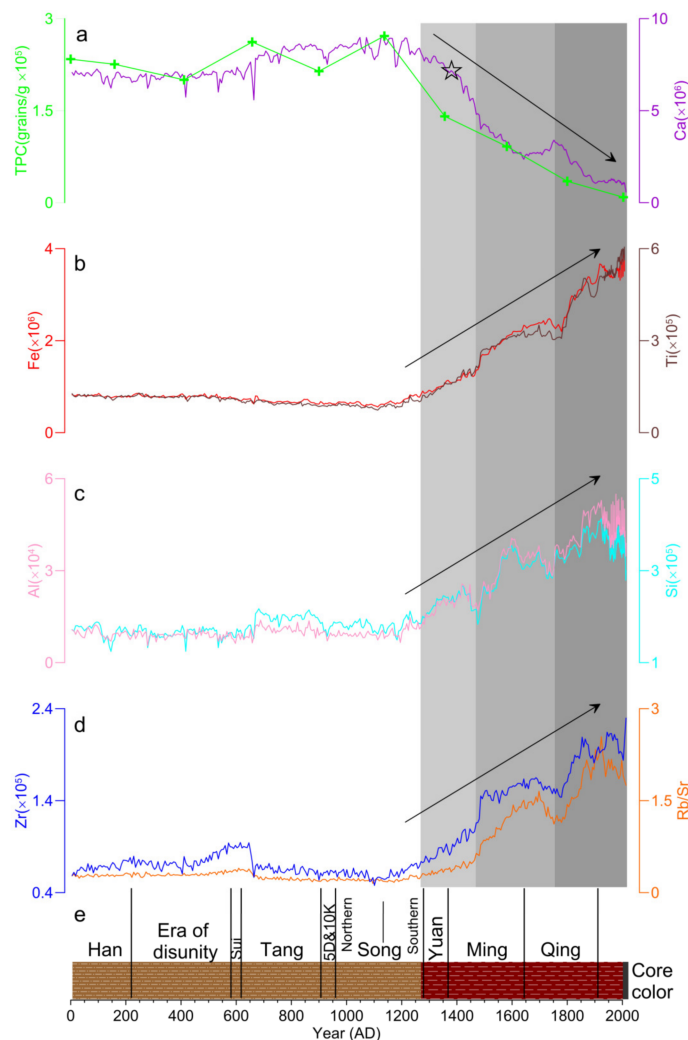


Figure 5. Proxies from YZH-1 over the last 2000 years: (a) Total pollen concentration [3] (TPC, green line) and Ca values (purple line), the symbol ☆ represents the era in which the Tangchi Canal was constructed; (b) values of Fe (red line) and Ti (brown line); (c) Al values (pink line) and Si values (cyan line); (d) Zr values (blue line) and ratio of Rb to Sr (orange line); (e) lithology and color of YZH-1 core, black lines are the Chinese dynasties. Gray bars indicate the gradual increasingly intensive human impact on the lake.

5. Conclusions

Using multivariate statistical analysis, we classified the sediment elements of Lake Yangzong into two main categories: The first category includes elements such as Fe, Ti, Rb, Zr, Al, Mn, and Si, which originate from exogenous detrital matter and reflect the intensity of basin erosion. These elements can serve as valuable proxy indicators for changes in the basin environment and human-activity intensity. The second category comprises elements Ca and Sr, representing endogenous substances generated by chemical and biological processes within the lake. Two principal component analysis (PCA) axes indicate the elemental variations in the Lake Yangzong sediments, with PC1 explaining 78.4% of the elemental data, reflecting the variation between exogenous input detrital minerals and authigenic minerals in the lake.

From 13,400 to 680 cal a BP, the main components, including exogenous detrital elements and variations in organic matter content, correspond to the stages of climate evolution. These components are primarily controlled by climate and vegetation conditions. During colder periods, erosion intensity is higher, and proxy indicators show elevated values. In warmer periods, erosion weakens, and human activity during this time is not significant, resulting in a minimal impact on basin vegetation coverage and erosion intensity. During the Yuan dynasty (680 cal a BP, AD 1271), there was a significant shift in the state's territorial views and border governance strategies. After establishing a province in Yunnan, the Yuan dynasty encouraged settlement, expanded the Yunnan passage, strengthened connections with the mainland, and saw a large influx of immigrants from other provinces into Yunnan. The population and cultivated land area in Yunnan increased significantly, causing tense human–environment relationships. Vegetation destruction in the watershed accelerated soil erosion, contributing to a significant increase in the content of elements such as Fe, Ti, Rb, Zr, Al, Mn, and Si in the drill core sediments of Lake Yangzong. The carbon sequestration capacity of the Lake Yangzong watershed significantly decreased, making it a potential carbon source. In the year AD 1388 (562 cal a BP), the excavation of the Tangchi Canal caused a significant transformation in the hydrological environment of Lake Yangzong, changing it from an endorheic lake to an exorheic lake. The lake water shifted from being consumed by evaporation to being lost through outflow combined with evaporation. As a result, Ca ions were lost through the Tangchi Canal, making it difficult to reach supersaturation and form precipitates. This led to a fundamental change in the water–carbon cycle pattern in the Lake Yangzong basin. This study lacks sufficient ¹⁴C dating data and pollen data that directly reflect human activities, and different carbon isotope compositions in the sediment were not distinguished, which should be a focus of future research.

Author Contributions: Conceptualization, H.Z. and H.L. (Huayong Li); methodology, H.L. (Huayong Li); software, Y.J. and D.L.; formal analysis, L.D.; investigation, H.Z., H.L. (Huayong Li), L.D. and H.L. (Huayu Li); resources, H.Z.; data curation, Y.J., X.S. and Z.L.; writing—original draft preparation, H.L. (Huayong Li); writing—review and editing, H.Z.; visualization, H.L. (Huayu Li) and D.L.; project administration, H.Z.; funding acquisition, H.Z. and H.L. (Huayong Li). All authors have read and agreed to the published version of the manuscript.

Funding: This research was financially supported by the National Natural Science Foundation of China (Grant No. 41807447); Henan Provincial Science and Technology Research Project (Grant No. 232102321109); Foundation for Distinguished Young Talents in Higher Education of Henan (Grant No. 2023GGJS125); Key Scientific Research Project of Colleges and Universities in Henan Province (Grant No. 24A170002); and Science and Technology Research Project of Anyang City (Grant No. 2023C01SF195).

Data Availability Statement: Research data from this study are available on request (zhanghc@ynu.edu.cn).

Acknowledgments: We thank Yang Pu, Linpei Huang, Hongwei Meng, Yang Zhang, Han Wu, and the graduate students who participated in the field works and laboratory analyses.

Conflicts of Interest: The authors declare no conflict of interest.

References

1. Li, Q.; Wang, Y.; Li, L.; Zhang, H.; Wang, B. Ecological restoration scheme of lake basins on the karst plateau based on natural solution: Take nine lakes on the Yunnan Plateau as example. *Carsologica Sin.* **2023**, *42*, 391–401.
2. Chen, F.H.; Chen, X.M.; Chen, J.H.; Zhou, A.F.; Wu, D.; Tang, L.Y.; Zhang, X.J.; Huang, X.Z.; Yu, J.Q. Holocene vegetation history, precipitation changes and Indian Summer Monsoon evolution documented from sediments of Xingyun Lake, south-west China. *J. Quat. Sci.* **2014**, *29*, 661–674. [[CrossRef](#)]
3. Wang, M.; Meng, H.W.; Huang, L.P.; Sun, Q.F.; Sun, H.C.; Shen, C.M. Vegetation succession and forest fires over the past 13000 years in the catchment of Yangzonghai Lake, Yunnan. *Quat. Sci.* **2020**, *40*, 175–189.
4. Li, H.J.; Chong, D.; Fan, S.; Zhang, S.Q.; Wang, J. Remote sensing monitoring of the nine plateau lakes' surface area in Yunnan in recent thirty years. *Resour. Environ. Yangtze Basin* **2016**, *25*, 32–37.

5. Li, J.L.; Li, H.Y.; Luo, L.C.; Gong, F.L.; Zhang, R.F.; Liu, F.L.; Wu, S.T.; Luo, B.Y. Water level retrieval for the past and prediction for the next 30 years at Lake Fuxian. *Lake Sci.* **2022**, *34*, 958–971.
6. He, K.D.; Gao, W.; Duan, C.Q.; Zhu, Y.G.; Pan, Y.; Liu, C.E.; Zhang, W.; Yang, G.Y. Water level variation and its driving factors in Lake Dianchi, Fuxian and Yangzong during 1988–2015. *Lake Sci.* **2019**, *31*, 1379–1390.
7. Hu, K.; Chen, G.J.; Huang, L.P.; Chen, X.L.; Liu, Y.Y.; Lu, H.B.; Tao, J.S.; Kang, W.G. Sediment records of extreme droughts and ecological consequences in Yuxian Lake, southeast Yunnan. *Acta Hydrobiol. Sin.* **2017**, *41*, 724–734.
8. Liu, Q.; Chang, F.Q.; Xie, P.; Zhang, Y.; Duan, L.Z.; Li, H.Y.; Zhang, X.N.; Zhang, Y.; Li, D.L.; Zhang, H.C. Microbiota assembly patterns and diversity of nine plateau lakes in Yunnan, southwestern China. *Chemosphere* **2022**, *314*, 137700. [[CrossRef](#)] [[PubMed](#)]
9. Crutzen, P.J. Geology of mankind. *Nature* **2002**, *415*, 23. [[CrossRef](#)] [[PubMed](#)]
10. Li, Y.; Fang, L.C.; Wang, Y.Z.; Mi, W.J.; Ji, L.; Zhang, G.X.; Yang, P.H.; Chen, Z.B.; Bi, Y.H. Anthropogenic activities accelerated the evolution of river trophic status. *J. Ecol. Indic.* **2022**, *136*, 108584. [[CrossRef](#)]
11. Zalasiewicz, J.; Waters, C.N.; Summerhayes, C.P.; Wolfe, A.P.; Barnosky, A.D.; Cearreta, A.; Crutzen, P.; Ellis, E.; Fairchild, I.J.; Gałuszka, A.; et al. The Working Group on the Anthropocene: Summary of evidence and interim recommendations. *Anthropocene* **2017**, *19*, 55–60. [[CrossRef](#)]
12. Waters, C.N.; Williams, M.; Zalasiewicz, J.; Turner, S.D.; Barnosky, A.D.; Head, M.J.; Wing, S.L.; Wagnreich, M.; Steffen, W.; Summerhayes, C.P.; et al. Epochs, events and episodes: Marking the geological impact of humans. *Earth-Sci. Rev.* **2022**, *234*, 104171. [[CrossRef](#)]
13. Liu, Y.L.; Zhang, E.L.; Liu, E.F.; Wang, R.; Yuan, H.Z.; Kong, D.P.; Zhou, Q.C. TOC and Black Carbon records in sediment of Lake Yangzong, Yunnan Province under the influence of human activities during the past century. *Lake Sci.* **2017**, *29*, 1018–1028.
14. Wang, R.; Zheng, W.X.; Xu, M.; Yang, H. The declines of heterogeneity and stability in diatom communities are associated with human activity. *Ecol. Evol.* **2023**, *13*, e10695. [[CrossRef](#)] [[PubMed](#)]
15. Liao, L.Y.; Sun, Q.F.; Yu, M.M.; Meng, H.W.; Wang, M.; Chen, G.J.; Shen, C.M. Vegetation, climate and fires in the West Lake basin of Dali, Yunnan, China since the Industrial Revolution. *Quat. Sci.* **2024**, *44*, 174–190.
16. Hillman, L.A.; Yao, A.; Abbott, B.M.; Bain, D.J. Two millennia of anthropogenic landscape modification and nutrient loading at Dian Lake, Yunnan Province, China. *Holocene* **2019**, *29*, 505–517. [[CrossRef](#)]
17. Hillman, L.A.; Abbott, B.M.; Yu, J.Q. Climate and anthropogenic controls on the carbon cycle of Xingyun Lake, China. *Palaeogeogr. Palaeoclimatol. Palaeoecol.* **2018**, *501*, 70–81. [[CrossRef](#)]
18. Li, K.; Liao, M.N.; Ni, J. Vegetation response to climate change and human activity in southwestern China since the Last Glacial Maximum. *Palaeogeogr. Palaeoclimatol. Palaeoecol.* **2024**, *636*, 111990. [[CrossRef](#)]
19. Zhang, Y.; Liu, L.; Li, P.; Hu, Y.P.; Li, L.J.; Su, Y.W.; Xing, X.L.; Feng, J.; Ye, T. Changes of organic C and N stable isotope and their environmental implication during the past 130 years of Chen Lake. *China Environ. Sci.* **2023**, *43*, 1307–1316.
20. Jin, Z.D.; Wang, S.M.; Shen, J.; Zhang, E.L.; Li, F.C.; Ji, J.F.; Lu, X.W. Chemical weathering since the Little Ice Age recorded in lake sediments: A high-resolution proxy of past climate. *Earth Surf. Process. Landf.* **2001**, *26*, 775. [[CrossRef](#)]
21. Wang, S.M.; Zhang, Z.K. New progress of lake sediments and environmental changes research in China. *Chin. Sci. Bull.* **1999**, *44*, 579–587. [[CrossRef](#)]
22. Wang, Y.B.; Xie, Y.; Liu, X.Q.; Shen, J.; Wang, Y.; Li, Z. Climate and human induced 2000-year vegetation diversity change in Yunnan, southwestern China. *Holocene* **2022**, *32*, 1327–1339. [[CrossRef](#)]
23. Bonk, A.; Piotrowska, N.; Żarczyński, M.; Enters, D.; Makohonienko, M.; Rzedkiewicz, M.; Tylmann, W. Limnological responses to environmental changes during the last 3000 years revealed from a varved sequence of lake Lubińskie (western Poland). *Catena* **2023**, *226*, 107053. [[CrossRef](#)]
24. Dionysios, S.; Alexandros, E.; Alessia, M.; Adam, L.; Pavlos, A. Holocene Hydroclimatic Changes in Northern Peloponnese (Greece) Inferred from the Multiproxy Record of Lake Lousoi. *Water* **2022**, *14*, 641.
25. Sebastien, B.; Tjallingii, R.; Kylander, M.E.; Wilhelm, B.; Roberts, S.J.; Arnaud, F.; Brown, E.; Bindler, R. Inorganic geochemistry of lake sediments: A review of analytical techniques and guidelines for data interpretation. *Earth-Sci. Rev.* **2024**, *249*, 104639.
26. Kylander, M.E.; Ampel, L.; Wohlfarth, B.; Veres, D. High-resolution X-ray fluorescence core scanning analysis of Les Echets (France) sedimentary sequence: New insights from chemical proxies. *J. Quat. Sci.* **2011**, *26*, 109–117. [[CrossRef](#)]
27. Jansen, J.H.F.; Van der Gaast, S.J.; Koster, B.; Vaars, A.J. CORTEX, a shipboard XRF-scanner for element analyses in split sediment cores. *Mar. Geol.* **1998**, *141*, 143–153. [[CrossRef](#)]
28. Francus, P.; Lamb, H.; Nakagawa, T.; Marshall, M.; Brown, E. The potential of high-resolution X-ray fluorescence core scanning: Applications in paleolimnology. *PAGES News* **2009**, *17*, 93–96. [[CrossRef](#)]
29. Yang, H.E.; Zhao, Y.; Cui, Q.Y.; Ren, W.H.; Li, Q. Paleoclimatic indication of X-ray fluorescence core-scanned Rb/Sr ratios: A case study in the Zoige Basin in the eastern Tibetan Plateau. *Sci. China Earth Sci.* **2021**, *64*, 80–95. [[CrossRef](#)]
30. Liang, Q.S.; Zhang, W.X.; Lin, Y.J.; Wu, M.J.; Liu, T.T.; Wang, L.M.; Ma, S.R. Study on elemental characteristics of lacustrine sediments and catchment erosion of Fuxian lake in central Yunnan plateau. *China Environ. Sci.* **2020**, *40*, 1740–1747.
31. Sabatier, P.; Dezileau, L.; Colin, C.; Briquieu, L.; Bouchette, F.; Martinez, P.; Siani, G.; Raynal, O.; Grafenstein, U.V. 7000 years of paleostorm activity in the NW Mediterranean Sea in response to Holocene climate events. *Quat. Res.* **2012**, *77*, 1–11. [[CrossRef](#)]
32. Li, D.; Tan, L.C.; Guo, F.; Cai, Y.J.; Sun, Y.B.; Xue, G.; Cheng, X.; Yan, H.; Cheng, H.; Edwards, L.R.; et al. Application of Avaatech X-ray fluorescence core-scanning in Sr/Ca analysis of speleothems. *Sci. China Earth Sci.* **2019**, *62*, 964–973. [[CrossRef](#)]

33. Zhang, X.N.; Zhang, H.C.; Chang, F.Q.; Ashraf, U.; Peng, W.; Wu, H.; Liu, F.W.; Zhang, Y.; Duan, L.Z. Application of Corrected Methods for High-Resolution XRF Core Scanning Elements in Lake Sediments. *Appl. Sci.* **2020**, *10*, 8012. [[CrossRef](#)]
34. Hu, N.J.; Shi, X.F.; Huang, P.; Liu, J.H. Distribution of metals in surface sediments of Liaodong Bay, Bohai Sea. *China Environ. Sci.* **2010**, *30*, 380–388.
35. Lei, G.L.; Zhang, H.C.; Chang, F.Q.; Zhu, Y.; Li, C.H.; Xie, X.; Lei, Y.B.; Zhang, W.X.; Pu, Y. Comparison and correction of element measurements in lacustrine sediments using X-ray fluorescence core-scanning with ICP-OES method: A case study of Zigetang Co. *Lake Sci.* **2011**, *23*, 287–294.
36. Niu, J.; Zhang, W.X.; Zhang, H.C.; Duan, L.Z.; Wu, M.J.; Wang, L.M. The characteristics of geochemical elements in Fuxian Lake sediments and its environmental significance based on XRF core scanning. *Spectrosc. Spectr. Anal.* **2019**, *39*, 2223–2227.
37. Wu, Y.H.; Lücke, A.; Jin, Z.D.; Wang, S.M.; Schleser, H.G.; Battarbee, W.R.; Xia, W.L. Holocene climate development on the central Tibetan Plateau: A sedimentary record from Cuoe Lake. *Palaeogeogr. Palaeoclimatol. Palaeoecol.* **2006**, *234*, 328–340.
38. Jin, Z.D.; Cao, J.J.; Wu, J.J.; Wang, S.M. A Rb/Sr record of catchment weathering response to Holocene climate change in Inner Mongolia. *Earth Surf. Process. Landf.* **2006**, *31*, 285–291. [[CrossRef](#)]
39. Ma, X.Y.; Chen, D.; Yang, Y.P.; Zhang, Y.Z.; Zhang, J.W. Statistical Analysis of XRF Scanned Elements and Their Environmental Significance in Hala Lake, Qinghai, China. *J. Salt Lake Res.* **2014**, *22*, 1–10.
40. Evans, G.; Augustinus, P.; Gadd, P.; Zawadzki, A.; Ditchfield, A. A multi-proxy μ -XRF inferred lake sediment record of environmental change spanning the last ca. 2230 years from Lake Kanono, Northland, New Zealand. *Quat. Sci. Rev.* **2019**, *225*, 106000. [[CrossRef](#)]
41. Hardeng, J.; Bakke, J.; Cederstrøm, J.M.; Forsmo, J.; Haugen, T.A.; Sabatier, P.; Støren, E.W.N.; van der Bilt, W.G.M. A 7000-year record of extreme flood events reconstructed from a threshold lake in southern Norway. *Quat. Sci. Rev.* **2024**, *331*, 108659. [[CrossRef](#)]
42. Rohozin, Y.; Ljung, K. Palaeoenvironmental changes in eastern Crimea over the last 7600 years inferred from a multi-proxy study of a sediment archive from Lake Chokrak. *Holocene* **2024**, *34*, 175–188. [[CrossRef](#)]
43. Duxbury, L.C.; Johns-Mead, L.Y.; Cadd, H.; Francke, A.; Löhr, S.C.; Law, W.B.; Armbrrecht, L.; Hall, P.A.; Zawadzki, A.; Jacobsen, G.E.; et al. Holocene climate and catchment change inferred from the geochemistry of Lashmars Lagoon, Kangaroo Island (Karti/Karta), southern Australia. *Palaeogeogr. Palaeoclimatol. Palaeoecol.* **2024**, *634*, 111928. [[CrossRef](#)]
44. Wu, H.; Zhang, H.C.; Chang, F.Q.; Duan, L.Z.; Zhang, X.N.; Peng, W.; Liu, Q.; Zhang, Y.; Liu, F.W. Isotopic constraints on sources of organic matter and environmental change in Lake Yangzong, Southwest China. *J. Asian Earth Sci.* **2021**, *217*, 104845. [[CrossRef](#)]
45. Yang, X.Y.; Ren, S.C. Structure model of karst underground water system in Yangzonghai basin, Yunnan. *Yunnan Geol.* **2024**, *33*, 103–107.
46. Ming, Q.Z.; Tong, S.Y. *Yunnan Geography*; Beijing Normal University Press: Beijing, China, 2016; pp. 111–112.
47. Zheng, W.X.; Wang, R.; Zhang, E.L.; Cao, Y.M.; Kong, D.P. Diversity and stability dynamic of chironomid assemblages in the last two centuries of Lake Yangzong, Yunnan Province. *Lake Sci.* **2018**, *30*, 847–856.
48. Yu, M.M.; Meng, H.W.; Chen, J.L.; Sun, Q.F.; Shen, C.M. The radiocarbon reservoir effects of lakes in Yunnan. *Quat. Sci.* **2023**, *43*, 390–402.
49. Reimer, P.J.; Bard, E.; Bayliss, A.; Beck, J.W.; Blackwell, P.G.; Ramsey, C.B.; Brown, D.M.; Buck, C.E.; Edwards, R.L.; Friedrich, M.; et al. Selection and Treatment of Data for Radiocarbon Calibration: An Update to the International Calibration (IntCal) Criteria. *Radiocarbon* **2013**, *55*, 1923–1945. [[CrossRef](#)]
50. Yang, Y.P.; Ma, X.Y.; Wang, L.; Fu, X.; Zhang, Y.Z.; Zhang, J.W. Evaluation of three methods used in carbonate content determination for lacustrine sediments. *Lake Sci.* **2016**, *28*, 917–924.
51. Qin, R.; Liu, L.Y.; Wang, J.J.; Liu, X.Q.; Zhang, Q.; Feng, S.N. Application of XRF core scanning in varved lake sediments: A case study on Lake Xinluhai in the southeastern margin of Qinghai-Tibetan Plateau. *Lake Sci.* **2022**, *34*, 1723–1734.
52. Zhang, H.; Niu, L.L.; Yuan, Z.J.; Zhang, C.; Sun, H.L.; Zhang, X.J.; Zhou, A.F. Mid-late Holocene soil erosion record from lake deposit of Liupan Mountains. *J. Earth Environ.* **2021**, *12*, 146–158.
53. Li, K.; Tan, B.; Ni, J.; Liao, M.N. Hydroclimate changes since Last Glacial Maximum: Geochemical evidence from Yilong Lake, southwestern China. *Acta Ecol. Sin.* **2018**, *38*, 8973–8982.
54. Lan, M.W.; Song, Y.G.; Cheng, L.Q. Review on Formation of Lacustrine Carbonate Minerals and Their Paleoclimates Significance. *J. Earth Sci. Environ.* **2022**, *44*, 156–170.
55. Jin, Y.; Wang, Y.; Hu, J.; Han, R.C.; Xiang, C.S. Geochemical Element Records and Hydrological Significance of Lake Shengjin Sediments During the Past Millennium. *Acta Sedimentol. Sin.* **2023**, *41*, 219–232.
56. Li, W.C. Nitrogen accumulation in the sediment of East Taihu Lake and biological sedimentation of aquatic plants. *China Environ. Sci.* **1997**, *17*, 35–38.
57. Pu, Y.; Han, Y.; Zhang, H.C.; Chang, F.Q. Late Holocene climatic and environmental variation in the source area of the Yellow River recorded by sediments from the Lake Ngoring, northeastern Qinghai-Tibetan Plateau. *Quat. Sci.* **2021**, *41*, 1000–1011.
58. Lv, M.H.; Wang, H.Y.; Cai, Y.L.; Wang, W.B.; Xiu, L. Magnetic properties of core HF1-2 from Lake Hongfeng in Guizhou Province and its implications for soil erosion. *Lake Sci.* **2008**, *20*, 298–305.
59. Song, Y.L.; Chen, J.A.; Yang, H.Q.; Ding, W.; Tao, H.B.; Luo, J.; Wang, J.F. Distribution and Source of the Organic Matter in the Sediment of Fuxian Lake, Yunnan Province. *Bull. Mineral. Petrol. Geochem.* **2016**, *35*, 618–624+607.

60. Wu, J.; Shen, C.M.; Yang, H.; Qian, S.; Xie, S.C. Holocene temperature variability in China. *Quat. Sci. Rev.* **2023**, *321*, 108184. [[CrossRef](#)]
61. Li, M.J.; He, F.N.; Yang, F.; Li, S.C. Re-construction of cropland area at the provincial level in the early Yuan Dynasty. *Acta Geogr. Sin.* **2018**, *73*, 832–842.
62. Fang, T. The agriculture and agricultural taxes and levies of Yunnan province in the Yuan dynasty. *J. Yunnan Norm. Univ.* **2004**, *4*, 57–64.
63. Gu, Y.J. The Immigration to Yunnan Province in the Dynasties of Yuan, Ming and Qing. *Ethno-Natl. Stud.* **2003**, *2*, 69–78+109.
64. Li, T. Climate Change Since the 12 ka Recorded in the Sediments of Lake Fuxian. Master's Thesis, Yunnan Normal University, Kunming, China, 2019.
65. Yao, A.; Darré, V.; Jiang, Z.L.; Lam, W.C.; Yang, W. Bridging the time gap in the Bronze Age of Southeast Asia and Southwest China. *Archaeol. Res. Asia* **2020**, *22*, 100189. [[CrossRef](#)]
66. Liu, P.L.; Liu, F.W.; Li, G.; Li, Y.J.; Cao, H.H.; Li, X.R. Anthropogenic Impact on the Terrestrial Environment in the Lake Dian Basin, Southwestern China during the Bronze Age and Ming-Qing period. *Land* **2024**, *13*, 228. [[CrossRef](#)]
67. Martello, R.D. The origins of multi-cropping agriculture in Southwestern China: Archaeobotanical insights from third to first millennium B.C. Yunnan. *Asian Archaeol.* **2022**, *6*, 65–85. [[CrossRef](#)] [[PubMed](#)]
68. Gao, Y.; Dong, G.H.; Yang, X.Y.; Chen, F.H. A review on the spread of prehistoric agriculture from southern China to mainland southeast Asia. *Sci. China Earth Sci.* **2020**, *63*, 615–625. [[CrossRef](#)]
69. Wei, W.J.; Gui, Z.F.; Xue, B.; Duan, H.T.; Yao, S.C.; Li, X.X. Effects of land use changes on the carbon storage of terrestrial ecosystem—A case study of Hulun Lake and Taihu Lake basins. *Quat. Sci.* **2012**, *32*, 327–336.
70. Jiang, W.; Hou, Q.Y.; Yang, Z.F.; Xia, X.Q.; Zhong, C. Migration and Deposition Flux of Organic Carbon in the Wuyuerhe River Basin in Heilongjiang Province. *Geoscience* **2011**, *25*, 384–392.
71. Gao, Y.; Luo, B.; Shen, D.; Jia, J.J.; Lu, Y.; Wang, S.Y. Recognition and challenges of the inland water carbon source and sink processes on the Qinghai-Tibet Plateau. *Lake Sci.* **2023**, *35*, 1853–1865.

Disclaimer/Publisher's Note: The statements, opinions and data contained in all publications are solely those of the individual author(s) and contributor(s) and not of MDPI and/or the editor(s). MDPI and/or the editor(s) disclaim responsibility for any injury to people or property resulting from any ideas, methods, instructions or products referred to in the content.